# Evidence against the acidification hypothesis in cystic fibrosis

**Gregory A. Gibson, Warren G. Hill and Ora A. Weisz**

*Am J Physiol Cell Physiol* 279:C1088-C1099, 2000. ;

*Am J Physiol Cell Physiol*
279: C1088–C1099, 2000.

# Evidence against the acidification hypothesis in cystic fibrosis

GREGORY A. GIBSON,[1] WARREN G. HILL,[2] AND ORA A. WEISZ[1,2]
[1]*Laboratory of Epithelial Cell Biology, Renal-Electrolyte Division, and* [2]*Department of Cell Biology and Physiology, University of Pittsburgh, Pittsburgh, Pennsylvania 15261*

Received 22 February 2000; accepted in final form 24 April 2000

**Gibson, Gregory A., Warren G. Hill, and Ora A. Weisz.** Evidence against the acidification hypothesis in cystic fibrosis. *Am J Physiol Cell Physiol* 279: C1088–C1099, 2000.—The pleiotropic effects of cystic fibrosis (CF) result from the mislocalization or inactivity of an apical membrane chloride channel, the cystic fibrosis transmembrane conductance regulator (CFTR). CFTR may also modulate intracellular chloride conductances and thus affect organelle pH. To test the role of CFTR in organelle pH regulation, we developed a model system to selectively perturb the pH of a subset of acidified compartments in polarized cells and determined the effects on various protein trafficking steps. We then tested whether these effects were observed in cells lacking wild-type CFTR and whether reintroduction of CFTR affected trafficking in these cells. Our model system involves adenovirus-mediated expression of the influenza virus M2 protein, an acid-activated ion channel. M2 expression selectively slows traffic through the *trans*-Golgi network (TGN) and apical endocytic compartments in polarized Madin-Darby canine kidney (MDCK) cells. Expression of M2 or treatment with other pH perturbants also slowed protein traffic in the CF cell line CFPAC, suggesting that the TGN in this cell line is normally acidified. Expression of functional CFTR had no effect on traffic and failed to rescue the effect of M2. Our results argue against a role for CFTR in the regulation of organelle pH and protein trafficking in epithelial cells.

endosome; Golgi; Madin-Darby canine kidney

CYSTIC FIBROSIS (CF) results from the mislocalization or inactivity of the apical membrane cystic fibrosis transmembrane conductance regulator chloride channel (CFTR). In addition to its activity at the apical membrane of polarized cells, CFTR has also been postulated to modulate chloride conductances in acidified intracellular compartments and thereby regulate the pH of organelles along the secretory and endocytic pathways (2, 4). Comparison of the pH of the *trans*-Golgi network (TGN) and endosomal compartments in CF versus normal cells suggested that CF cells fail to adequately acidify these compartments (4). The consequences of disrupted Golgi and endosome pH in CF cells could include altered glycoconjugate composition at the cell surface [which could explain enhanced bacterial binding to CF cells (17, 39, 59, 60)] as well as altered membrane trafficking (4, 6, 10). However, the role of CFTR in modulating organelle pH and membrane trafficking has remained controversial for various reasons. One problem has been the lack of closely matched polarized CF and control cell lines in which to perform these studies. As a result, previous studies that examined the effect of CFTR on endosomal pH or membrane trafficking events were performed by using heterologous expression systems or nonpolarized CF and control cells (6, 10, 20, 21, 58, 62, 67). Although most of these studies found no effect of CFTR on either organelle pH or membrane trafficking, the presence of alternative chloride conductances in these systems could mask a functional requirement for CFTR. Another major complication in identifying the role of CFTR in regulating organelle pH is that the importance of acidification in protein traffic is not well understood. Previous studies employing global pH perturbants [such as weak bases or vacuolar $H^+$-ATPase (V-ATPase) inhibitors] to disrupt acidification have yielded conflicting results regarding the consequences of disrupting organelle acidification on biosynthetic and postendocytic traffic (16, 47, 49, 51, 73, 77, 78). Thus it has not been possible to correlate any differences in membrane traffic between CF and normal cells with a defect in acidification of CF cells.

We have generated a model system to selectively perturb the pH of a subset of acidified compartments in polarized epithelial cells. This system involves expression of the influenza virus M2 protein, an acid-activated proton-selective channel that increases the pH of a subset of acidified compartments in cells (14, 15, 26, 27, 30, 33, 42, 50, 54, 61, 68, 71, 74). We have previously demonstrated that expression of M2 disrupts acidification of the TGN and apical recycling endosomes, but not that of basolateral endosomes or lysosomes in polarized Madin-Darby canine kidney (MDCK) cells (31). Importantly, the TGN and apical endosomes are the same compartments whose pH is predicted to be disrupted in CF cells. Thus we asked whether M2 expression in polarized epithelial cells mimics the CF phenotype and whether expression of epitope-tagged, fully functional CFTR in cells lacking

Address for reprint requests and other correspondence: O. A. Weisz, Renal-Electrolyte Division, Univ. of Pittsburgh, 3550 Terrace St., Pittsburgh, PA 15261 (E-mail: weisz@msx.dept-med.pitt.edu).

The costs of publication of this article were defrayed in part by the payment of page charges. The article must therefore be hereby marked "*advertisement*" in accordance with 18 U.S.C. Section 1734 solely to indicate this fact.

  

functional chloride channel has any effect on biosynthetic or postendocytic traffic. Our previous data suggested that even closely matched CF and control cells are inappropriate for comparing protein processing/glycosylation to determine the function of CF (40). Therefore, we used recombinant adenoviruses to generate matched CFTR-expressing and -nonexpressing cell lines that differ only by overnight culture. We used two cell lines for our studies: MDCK II, which form sealed monolayers on permeable filter supports, and CFPAC, a pancreatic adenocarcinoma cell line that forms polarized islands of cells; neither of these cell lines express endogenous wild-type CFTR (46, 64).

## MATERIALS AND METHODS

*Cell lines.* Low-passage MDCK cells (type II) were maintained in minimal essential medium (Cellgro; Fisher Scientific, Pittsburgh, PA) supplemented with 10% fetal bovine serum (Atlanta Biologicals, Norcross, GA), streptomycin (100 μg/ml), and penicillin (100 U/ml). Generation and characterization of the MDCK T23 cell line, which stably expresses the tetracycline-repressible transactivator tTA (25), was described previously (5). These cells also express the polymeric immunoglobulin receptor (pIgR) under control of the butyrate-inducible cytomegalovirus promoter. By indirect immunofluorescence, >90% of the cells express detectable levels of pIgR after overnight induction with 2 mM butyrate. For all experiments, cells were seeded at high density ($\sim 2 \times 10^5$ cells/well) in 12-mm Transwells (0.4-μm pore; Costar, Cambridge, MA) for 2–3 days before infection with recombinant adenovirus. Experiments were performed the following day. CFPAC cells were obtained from American Type Culture Collection (Rockville, MD) and maintained in DMEM/F-12 supplemented with 10% fetal bovine serum. Cells were plated in 35-mm dishes ($3 \times 10^5$ cells/dish) or 12-well dishes ($1 \times 10^5$ cells/well) 2–3 days before infection.

*Recombinant adenoviruses.* The generation of E1-substituted recombinant adenoviruses (AV) encoding M2 in the correct and reverse orientations (AV-M2 and AV-M2rev, respectively) and influenza hemagglutinin (AV-HA) was described previously (31). Generation of an adenovirus encoding the rabbit pIgR was also described previously (32). Construction of AV-M2901, which encodes fully functional, epitope-tagged CFTR (M2–901/CFTR; Refs. 36 and 65) was described previously (37). Viruses were purified as described previously (31).

*Adenoviral infection.* Viral infection of filter-grown MDCK T23 cells was performed as described previously (31). CFPAC cells grown on plastic dishes were washed with a large volume of calcium-free phosphate-buffered saline (PBS) containing 1 mM $MgCl_2$ (PBS-M). After 5 min at room temperature, the PBS-M was replaced with a small volume (0.4 ml for 35-mm dishes, 0.3 ml for 12-well plates) of PBS-M containing recombinant adenovirus(es). The dishes were rocked briefly by hand, and the cells were returned to an incubator for 1–2 h. Mock-infected cells were treated identically except that virus was omitted during the incubation period. Dishes were then rinsed with PBS-M, and cells were incubated overnight in growth medium containing 2 mM butyrate.

*Indirect immunofluorescence.* Indirect immunofluorescence of fixed, virally infected cells was performed as described previously (34). Briefly, cells were rinsed once with PBS, fixed for 20 min at ambient temperature in 3% paraformaldehyde, and then incubated briefly with PBS containing 10 mM glycine and 0.02% sodium azide (PBS-G). Cells were permeabilized for 3 min in 0.5% Triton X-100 in PBS-G. Nonspecific binding was blocked with 0.25% ovalbumin in PBS-G before incubation with antibodies. M2 was detected using the monoclonal antibody 5C4 (1:250 dilution). Samples were then incubated with Cy3-conjugated affinity-purified goat anti-mouse antibody (2 mg/ml, 1:1,000 dilution; Jackson ImmunoResearch Laboratories, Avondale, PA). ZO-1 was detected using a polyclonal anti-ZO-1 antibody (Zymed Laboratories, South San Francisco, CA), followed by FITC-conjugated goat anti-rabbit IgG (2 mg/ml, 1:100 dilution; Jackson ImmunoResearch Laboratories). For live-cell staining of epitope-tagged CFTR, cells were rapidly chilled to 0°C by being washed with ice-cold PBS and were maintained on ice throughout the staining. Nonspecific binding sites were blocked by incubation for 20 min with 5% normal goat serum in PBS, and the cells were sequentially incubated with monoclonal anti-FLAG antibody (Stratagene, La Jolla, CA) and Cy3-conjugated goat anti-mouse secondary antibody for 30 min each with several washes in between. After cells were washed further, they were fixed for 10 min at 0°C and then 20 min at ambient temperature with 3% paraformaldehyde. Cells were viewed with a Nikon Optiphot microscope (Fryer, Carpentersville, IL), and images were acquired with a Hamamatsu C5985 chilled coupled charge-device camera (8 bit, 756 × 483 pixels; Hamamatsu Photonics Systems, Bridgewater, NJ) and printed with a Kodak 8650PS dye-sublimation printer (Rochester, NY).

*Transcytosis and recycling assays.* Recycling and transcytosis assays in filter-grown MDCK T23 cells were performed essentially as described previously (31). To measure recycling of IgA in CFPAC cells, virally infected cells in 12-well dishes were rinsed with MEM/BSA (minimum essential medium, Hanks' balanced salt solution, 0.6% BSA, and 20 mM HEPES, pH 7.4) and then incubated with 0.3 ml of MEM/BSA containing $^{125}$I-labeled IgA for 30 min at 37°C. Cells were rinsed once with MEM/BSA and washed three times for 5 min each with MEM/BSA on ice, the medium was replaced with prewarmed MEM/BSA, and the cells were returned to 37°C. At the designated time points, the media were collected and replaced. After the final time point, cells were solubilized and the amount of $^{125}$I-IgA in all samples was determined using a gamma counter (Packard Instrument, Downers Grove, IL). An equal number of mock-infected CFPAC cells (not expressing the pIgR) were treated identically to determine nonspecific IgA uptake and recycling, and these values were subtracted from the experimental samples. Where indicated, 10 μM forskolin (FSK; Calbiochem, San Diego, CA) was added during the last 10 min of radioligand uptake and included in subsequent steps. Recycling of $^{125}$I-labeled iron-loaded human transferrin (Tf) was performed as described above except that cells were preincubated in MEM/BSA for 45 min before $^{125}$I-Tf uptake for 45 min at 37°C. After cells were washed, they were incubated at 37°C for 3 min, the medium was replaced, and the time course was initiated.

*TGN-to-cell surface delivery of influenza HA.* Surface delivery of newly synthesized HA was performed essentially as described previously (31). Filter-grown T23 cells were coinfected with AV-HA [multiplicity of infection (MOI) 25] and AV-M2rev, AV-M2, or AV-M2901 (MOI 250). Plastic-grown CFPAC cells were coinfected with AV-HA (MOI 250), AV-TA (MOI 200), and AV-M2rev, AV-M2, or AV-M2901 (MOI 500) as described in *Adenoviral infection*. The following day, cells were rinsed once with PBS and then starved for 30 min in *medium A* (cysteine-free, methionine-free MEM containing 0.35g/l $NaHCO_3$, 10 mM HEPES, and 10 mM MES, pH 7.0). Where indicated, the M2 ion channel blockers amantadine (AMT; 5 μM; Sigma Chemical, St. Louis, MO), BL-1743 (10

μM), or the V-ATPase inhibitor bafilomycin $A_1$ ($BafA_1$, 1 μM; Sigma Chemical) were added at the beginning of the starvation and included during the pulse and chase periods. Cells were metabolically labeled with 50–100 μCi/ml [$^{35}$S]Express (NEN, Boston, MA) in the same medium and then chased for 2 h at 19°C in the same medium supplemented with four times the normal amount of cysteine and methionine (*medium B*). At various times, individual filters or dishes were removed, rapidly chilled to 0°C by being rinsed with ice-cold PBS, and incubated on ice for 30 min in 1 ml of *medium B* containing 100 μg/ml L-1-tosylamido-2-phenylethyl chloromethyl ketone-treated trypsin (Sigma Chemical) for 30 min. Trypsin cleaves HA into two subunits (HA1 and HA2) that remain associated via disulfide bonds during immunoprecipitation. Only the apical chamber of filter-grown cells was treated with trypsin. Trypsinization was stopped by incubating the cells twice for 10 min with ice-cold *medium B* containing 200 μg/ml soybean trypsin inhibitor (Sigma Chemical). Cells were rinsed with PBS and lysed in 0.5 ml of detergent solution (50 mM Tris·HCl, 2% NP-40, 0.4% deoxycholate, and 62.5 mM EDTA, pH 8.0) containing 1 μg/ml aprotinin and 20 μg/ml soybean trypsin inhibitor. Lysates were centrifuged briefly to remove nuclei, and SDS was added to the supernatant to a final concentration of 0.2%. HA was immunoprecipitated with the use of a monoclonal antibody, and antibody-antigen complexes were collected with the use of fixed *Staphylococcus aureus* (Pansorbin; Calbiochem) and washed three times with radioimmunoprecipitation assay (RIPA) buffer (10 mM Tris·HCl, 0.15 M NaCl, 1% Triton X-100, 1% NP-40, and 0.1% SDS, pH 7.4). After electrophoresis was carried out on 10% SDS-polyacrylamide gels, the percentage of cleaved HA was quantitated using a phosphorimager (GS-363 Molecular Imager System; Bio-Rad, Hercules, CA).

*Immunoprecipitation of virally expressed M2.* CFPAC cells were mock infected or infected with AV-M2 as described in *Adenoviral infection.* The following day, cells were rinsed once with PBS, starved for 30 min in *medium A*, and then radiolabeled in a humidified chamber for 2 h by placing the filters on a 25-μl drop of *medium A* containing 1.5 mCi/ml [$^{35}$S]Express. After labeling was completed, filters were rinsed once with PBS and then cut out of the plastic insert, and the cells were solubilized with 0.5 ml of 60 mM octylglucoside and 0.1% SDS in HEPES-buffered saline (10 mM HEPES and 0.15 M NaCl, pH 7.4) containing 1 μg/ml aprotinin. Lysates were centrifuged for 7 min at 16,000 *g* at room temperature, and the supernatants were immunoprecipitated with 5C4. Antibody-antigen complexes were collected with the use of fixed *S. aureus* (Pansorbin) and washed three times with RIPA buffer. After samples were eluted in Laemmli sample buffer, they were electrophoresed on 12% SDS-polyacrylamide gels and analyzed using a phosphorimager.

*Detection of functional epitope-tagged CFTR using SPQ.* cAMP-dependent anion efflux was monitored by 6-methoxy-*N*-(3-sulfopropyl)quinolinium (SPQ; Molecular Probes, Eugene, OR) fluorescence changes in living cells as described previously (40). Subconfluent cells grown on 25-mm glass coverslips were loaded with 10 mM SPQ in hypotonic NaI buffer. Iodide binds to SPQ and quenches its fluorescence. Cells were mounted in a perfusion chamber placed in a heating stage set to 37°C and perfused with buffers throughout the experiment. Imaging was performed on a Nikon Diaphot 300 inverted microscope equipped with a ×40 oil-immersion objective, an image intensifier, and a video camera. Excitation was at 330 nm, and image acquisition and analysis were performed by using Metafluor software (Universal Imaging, West Chester, PA). The average fluorescence intensity of individual cells in a field was monitored every 15 s throughout the assay. Cells were perfused for 2 min with isotonic NaI buffer, for 4 min with nitrate buffer to assess the rate of iodide leakage/exchange from nonstimulated cells, for 4 min with nitrate buffer supplemented with 10 μM FSK and 200 μM 3-isobutyl-1-methylxanthine (IBMX; Calbiochem), and then for 4 min with iodide buffer to requench intracellular SPQ. Functional CFTR was detected as an increase in the rate of dequenching of SPQ upon addition of FSK/IBMX. Assays on mock-infected and AV-M2901-infected cells were performed blindly.

## RESULTS

*Adenovirus-mediated expression of CFTR and M2 in polarized MDCK cells.* We used indirect immunofluorescence to confirm that polarized MDCK T23 cells were efficiently infected with recombinant adenoviruses encoding M2 or epitope-tagged CFTR. Filter-grown cells were infected with AV-M2 or AV-M2901 at an MOI of 250 and processed for indirect immunofluorescence the following day (Fig. 1). Approximately one-half of the cells expressed detectable levels of M2 or CFTR under these conditions. Previous experiments in which M2-expressing cells were infected under identical conditions gave maximal effects on all transport steps measured, although M2 could be detected in only 10–70% of the cells (31). In addition, infection of these cells with 10-fold lower levels of recombinant adenovirus that encodes influenza HA resulted in >90% expressing cells (31). Thus we suspect that essentially all

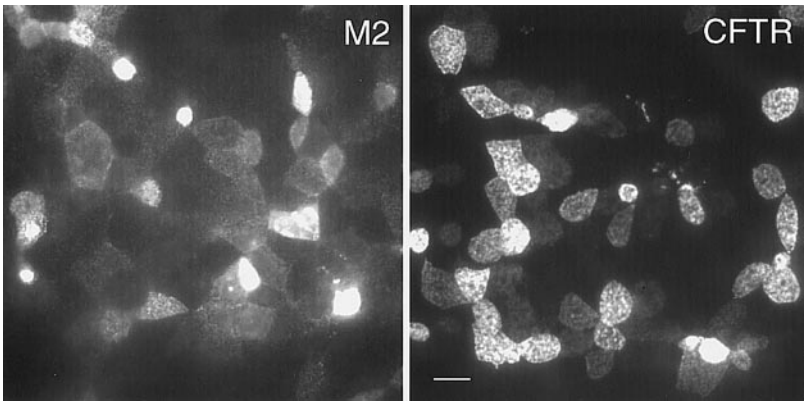


Fig. 1. Expression of M2 and epitope-tagged cystic fibrosis transmembrane conductance regulator (CFTR) in Madin-Darby canine kidney (MDCK) T23 cells. Filter-grown MDCK T23 cells were infected with adenoviruses encoding M2 (AV-M2) or M2901 (AV-M2901) at a multiplicity of infection (MOI) of 250. On the following day, cells expressing M2 were fixed and processed for indirect immunofluorescence, whereas cells expressing M2901 were processed for live-cell staining using anti-FLAG antibody as described in MATERIALS AND METHODS. Scale bar: 10 μm.

of the cells on the filter insert are infected under our conditions but that immunofluorescence detection of M2 and CFTR is not as sensitive as detection of HA.

*M2 but not CFTR slows protein traffic in polarized MDCK cells.* Although CFTR has been postulated to regulate TGN pH, the role of counterion conductance in regulating organelle acidification is controversial (3, 18, 44). We and others have previously determined that expression of M2, which increases TGN pH, inhibits surface delivery of newly synthesized HA in HeLa cells (33, 34, 61) as well as in polarized MDCK cells (32). The effect of M2 occurs at the level of HA exit from the TGN and is inhibited by inclusion of the ion channel blocker AMT (33, 34). The role of counterion conductance in regulating organelle acidification is controversial (3, 18, 44). By contrast, expression of CFTR might be expected to enhance acidification of the TGN, with unpredictable consequences on protein traffic through this compartment. Therefore, we compared the effects of M2 and CFTR on apical biosynthetic traffic in MDCK T23 cells. Polarized MDCK cells expressing HA and either M2 or CFTR were radiolabeled and chased for 2 h at 19°C to accumulate newly synthesized HA in the TGN (45). Control cells were infected with an adenovirus encoding M2 in the reverse orientation (M2rev) in addition to HA to maintain a constant MOI in all samples. Cells were then rapidly warmed, and the rate of HA delivery to the apical cell surface was quantitated (Fig. 2). As expected, M2 slowed the rate of HA delivery to the apical surface. The effect of M2 on this step in HA transport was similar to that of the V-ATPase inhibitor $BafA_1$ (Fig. 2, compare upright and inverted triangle symbols) and was blocked by inclusion of AMT during the experiment (not shown). However, expression of epitope-tagged CFTR (Fig. 2, square symbols) had no effect on the rate of HA delivery to the cell surface.

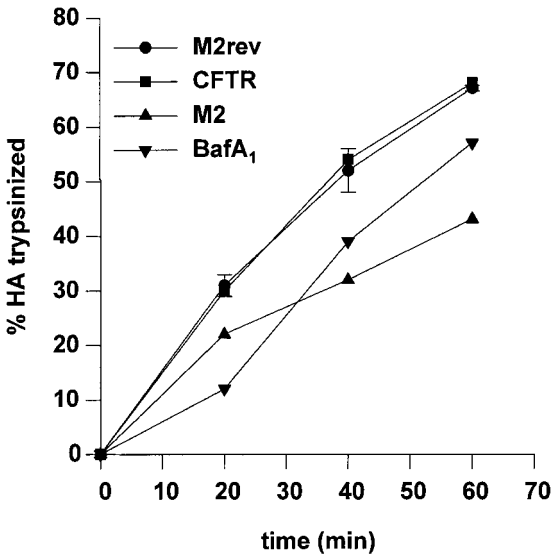


Fig. 2. Expression of M2 but not CFTR slows apical delivery of hemagglutinin (HA) in polarized MDCK cells. MDCK T23 cells were infected with AV-M2rev, AV-M2, or AV-M2901 as described in MATERIALS AND METHODS. On the following day, cells were starved for 30 min in cysteine-free, methionine-free medium, radiolabeled for 15 min, and then chased for 2 h at 19°C. Bafilomycin $A_1$ ($BafA_1$; 1 μM) was included in 1 set of AV-M2rev-infected cells at the beginning of the starvation period and in subsequent steps. The medium was replaced with prewarmed chase medium, and the cells were incubated at 37°C for the indicated times before rapid chilling and cell surface trypsinization. Cells were solubilized, HA was immunoprecipitated, and the percentage of cleaved HA was quantitated from SDS-PAGE gels with the use of a phosphorimager. Similar results were obtained in 3 experiments.

Next, we investigated the effect of epitope-tagged CFTR on the rate of postendocytic trafficking of preinternalized IgA in these cells. In polarized MDCK cells, newly synthesized pIgR is delivered to the basolateral surface, where it can bind IgA. The receptor is then transcytosed across the cell and cleaved to release IgA bound to a portion of the receptor into the apical medium. The remaining uncleaved receptor can recycle at the apical surface. Sensitive assays are available to measure the rate of IgA transcytosis and apical recycling, and we previously demonstrated that M2 expression slows the rate of both of these pathways in an AMT-inhibited manner (31). This suggests that both transcytosis and apical recycling are sensitive to altered organelle pH. We therefore compared the effects of M2 and CFTR expression on IgA transcytosis (Fig. 3). Unlike M2 expression, which inhibited the rate of transcytosis of IgA (Fig. 3*A*), CFTR expression had no effect on the rate of basolateral-to-apical transcytosis of IgA (Fig. 3*B*). In addition, because elevation of intracellular cAMP levels has previously been reported to stimulate the rate of IgA transcytosis across MDCK monolayers (29) and also activates CFTR channel activity, we tested whether stimulation of cAMP production by FSK would unmask an effect of CFTR in this assay (Fig. 3*B*). Although transcytosis was stimulated in all samples treated with FSK, we did not detect any difference between control and CFTR-expressing samples.

As an additional test to determine whether CFTR expression affects apical postendocytic traffic in polarized MDCK T23 cells, we measured the effects of CFTR and M2 expression on the apical recycling of preinternalized IgA. As previously demonstrated, expression of M2 had a modest but reproducible effect on the rate of apical recycling of IgA (Fig. 4*A*). By contrast, expression of CFTR in the presence (Fig. 4*B*) or absence (not shown) of FSK stimulation had no effect on the rate of IgA recycling.

*Expression of functional CFTR in CFPAC cells.* MDCK II cells do not express endogenous CFTR, yet they are able to acidify both apical and basolateral endocytic compartments to a similar extent (Dunn K, personal communication). Together with the experiments described above, these data suggest that exogenous expression of CFTR does not affect pH regulation in these cells. However, it could be argued that MDCK cells use an alternative mechanism to regulate organelle pH but that CFTR fulfills this function in cells that normally express the protein. Therefore, we tested the effect of CFTR expression on protein traffic in the CF cell line CFPAC, derived from a pancreatic adenocarcinoma from a CF patient (64). If the acidification

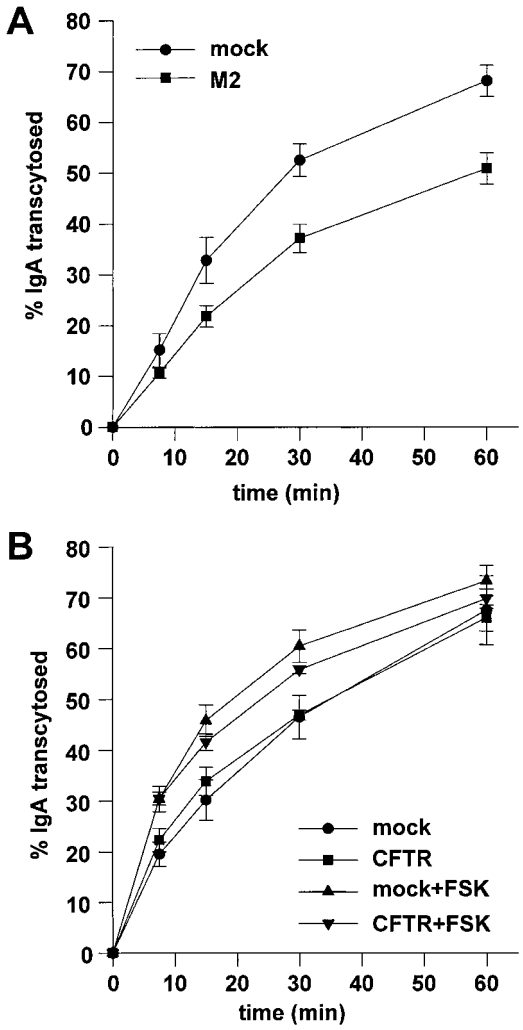


Fig. 3. M2 but not CFTR expression slows immunoglobulin A (IgA) transcytosis across MDCK monolayers. Filter-grown MDCK T23 cells were mock infected or infected with AV-M2 (*A*) or AV-M2901 (*B*), and cells were incubated overnight with 2 mM butyrate to induce expression of polymeric immunoglobulin receptor. Cells were incubated with basolaterally added $^{125}$I-labeled IgA for 10 min and then washed extensively. The rate of basolateral-to-apical transcytosis of $^{125}$I-IgA was quantitated as described in MATERIALS AND METHODS. Forskolin (FSK) was added to the indicated samples at the beginning of the IgA uptake period and was included during subsequent steps. Values are means ± SD for triplicate samples. Similar results were obtained in at least 3 independent experiments for each condition.

hypothesis is correct, organelles in CFPAC cells should be relatively alkaline, and expression of functional CFTR in CFPAC cells should stimulate both biosynthetic and postendocytic transport. By contrast, expression of M2 or incubation with global pH perturbants might be expected to have little or no effect on traffic in these cells. In our hands, these cells do not form confluent monolayers when grown on permeable filter supports; however, cells grown on plastic form large islands of relatively flat cells connected by tight junctions, suggesting that they are somewhat polarized (Fig. 5*C*). Infection of these cells with AV-M2901 resulted in high levels of CFTR expression (Fig. 5*B*) and restored FSK-stimulated halide-transport in these cells as measured using the SPQ assay (Fig. 6). Infection of these cells with AV-M2 resulted in nearly undetectable fluorescence labeling (not shown), perhaps because of the large size of these cells, but M2 could be readily immunoprecipitated from AV-M2-infected CFPAC cells (Fig. 5*D*).

*CFTR expression does not affect protein traffic in CFPAC cells.* To determine whether expression of M2 or CFTR affects biosynthetic traffic in CFPAC cells, we quantitated the kinetics of HA delivery from the TGN to the plasma membrane in AV-infected cells (Fig. 7*A*). Expression of active M2 decreased the rate of HA cell surface delivery, and the effect of M2 was completely reversed by AMT, suggesting that the effect of M2 was

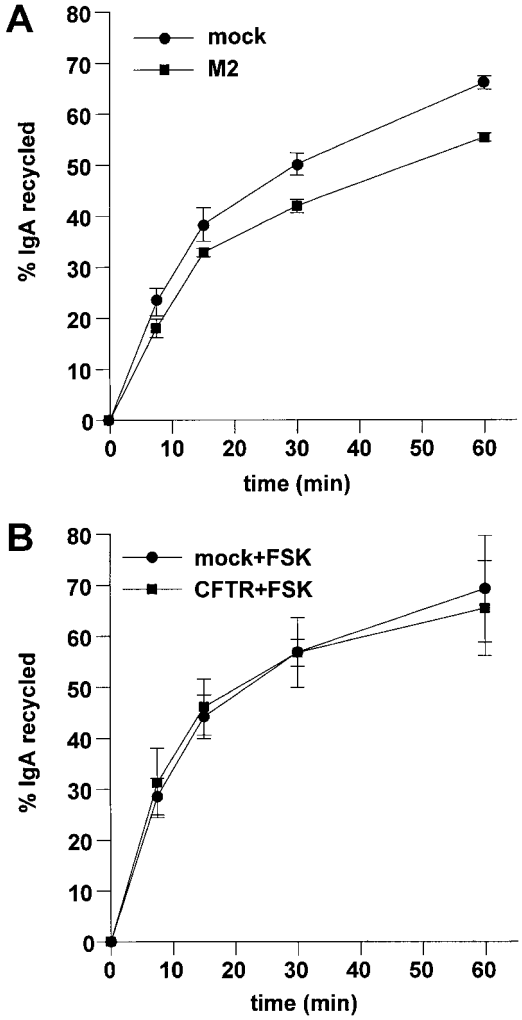


Fig. 4. M2 but not CFTR expression slows apical recycling of IgA in polarized MDCK cells. Filter-grown MDCK T23 cells were mock infected or infected with AV-M2 (*A*) or AV-M2901 (*B*), and cells were induced with 2 mM butyrate. On the following day, cells were incubated with apically added $^{125}$I-IgA for 10 min and then washed extensively. The rate of $^{125}$I-IgA apical recycling was quantitated as described in MATERIALS AND METHODS. FSK was added to the samples shown in *B* at the beginning of the IgA uptake period and was included during subsequent steps. Values are means ± SD for triplicate samples. Similar results were obtained in at least 3 independent experiments for each condition.

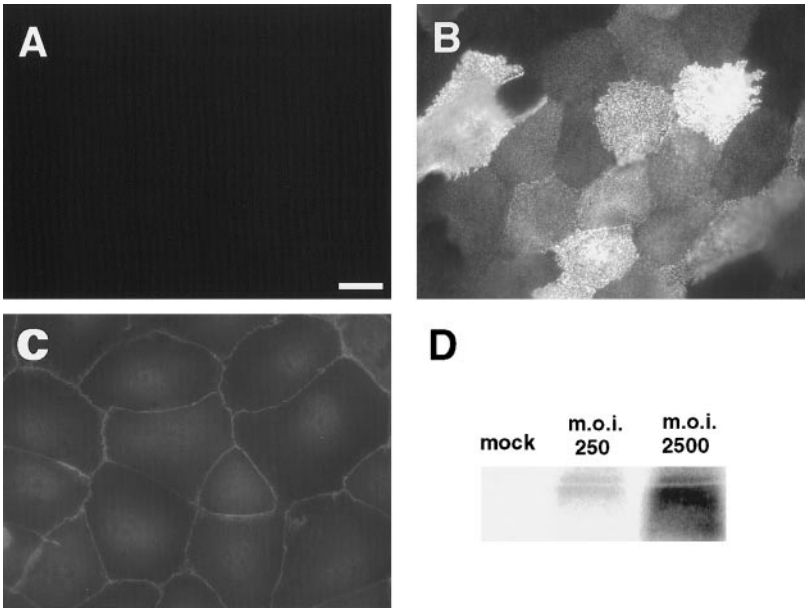


Fig. 5. Expression of CFTR in CFPAC cells (a cystic fibrosis pancreatic adenocarcinoma cell line). CFPAC cells plated on glass coverslips were mock infected (*A*) or infected with AV-M2901 (MOI 250; *B*) and induced with 2 mM butyrate. On the following day, cells were rapidly chilled and processed for live-cell staining with the use of anti-FLAG antibody as described in MATERIALS AND METHODS. *C*: AV-infected CFPAC cells were fixed and processed for indirect immunofluorescence to localize the tight junction marker ZO-1. *A–C*: scale bar, 10 μM. *D*: CFPAC cells were mock infected or infected with AV-M2 at an MOI of 250 or 2500. AV-transactivator (TA) was included at an MOI of 200. On the following day, cells were starved, radiolabeled for 3 h with 100 μCi/ml [$^{35}$S]cysteine and [$^{35}$S]methionine, and then solubilized and M2 immunoprecipitated.

due to altered TGN pH. Treatment with $BafA_1$ also decreased TGN-to-cell surface delivery kinetics of HA. By contrast, expression of epitope-tagged CFTR had no effect on the rate of HA delivery from the TGN to the cell surface. Interestingly, addition of FSK stimulated HA delivery kinetics in these cells, but the effect was independent of CFTR expression (Fig. 7*B*).

Because M2 alkalinizes compartments by essentially increasing the proton leak rate, it is possible that V-ATPase activity is actually increased in organelles that express M2. If V-ATPase activity were limited by lack of a counterion conductance in CFPAC cells, then CFTR expression might help drop the pH of these compartments in cells expressing M2. To test this possibility, we examined whether coexpression of CFTR would reverse the effects of M2 on HA cell surface delivery (Fig. 8). As we previously observed, M2 expression inhibited the amount of HA delivered to the plasma membrane during a 60-min chase period. Inhibition of M2 ion channel activity using AMT or another selective inhibitor (BL-1743; Ref. 72) restored normal delivery. However, expression of CFTR did not rescue the effect of M2 on HA delivery. Together, these results suggest that M2 expression and $BafA_1$ treatment are able to alkalinize the TGN and that CFTR expression does not substantially alter TGN pH. Furthermore, cAMP-mediated stimulation of apical biosynthetic delivery is CFTR independent.

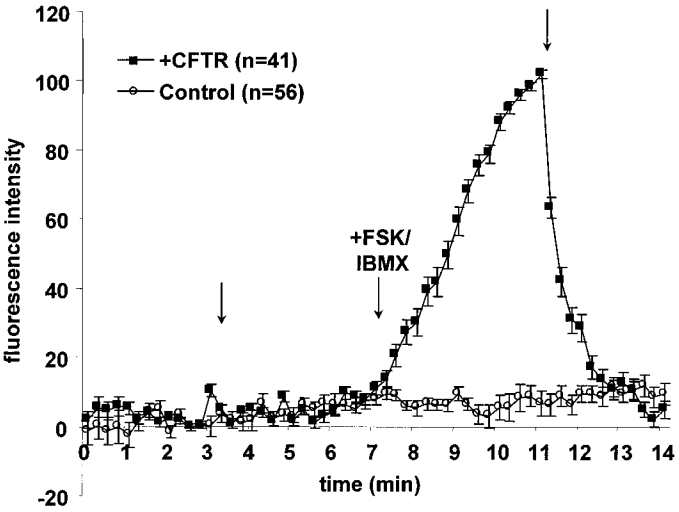


Fig. 6. CFTR expressed in CFPAC cells is functional. CFPAC cells were mock infected (control) or infected with AV-M2901 (+CFTR) at an MOI of 50. Cells were induced overnight with 2 mM butyrate and tested for expression of functional CFTR using the 6-methoxy-*N*-(3-sulfopropyl)quinolinium assay as described in MATERIALS AND METHODS. The arrows at 3, 7, and 11 min denote the switch to nitrate buffer, the addition of FSK and 3-isobutyl-1-methylxanthine (IBMX), and the return to iodide buffer, respectively.

We then determined the effects of M2 and CFTR expression on postendocytic traffic in CFPAC cells. Initially, we measured the effect of M2 and CFTR expression on the exocytosis of preinternalized $^{125}$I-IgA. Because the CFPAC cells grow in polarized islands, we have access to primarily the apical surface of these cells, although some basolateral surface is also accessible. Therefore, the IgA recycling assay actually reports a combination of recycling and transcytosis, which cannot be distinguished. Surprisingly, we found that neither M2 nor epitope-tagged CFTR expression affected the rate of exocytosis of preinternalized IgA in this assay (Fig. 9*A*). However, treatment with the global pH perturbant chloroquine resulted in significant inhibition of IgA exocytosis, suggesting a requirement for organelle acidification in either transcytosis or recycling in these cells. Increasing the level of M2 or CFTR expression by infection with 10-fold more virus (MOI 2,500) did not affect the results (not shown). In addition, inclusion of FSK did not stimulate exocytosis of preinternalized IgA in CFPAC cells under any conditions (Fig. 9*B*). Finally, we examined the effect of M2

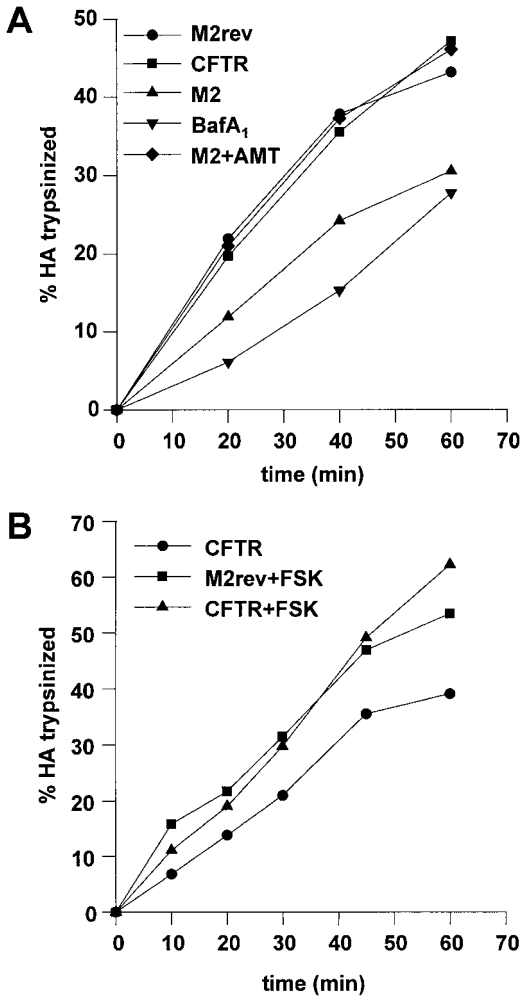


Fig. 7. M2 but not CFTR alters HA delivery in CFPAC cells. *A*: CFPAC cells were infected with AV-HA, AV-TA, and AV-M2rev, AV-M2901, or AV-M2 and induced with 2 mM butyrate. On the following day, cells were starved, radiolabeled for 15 min, and then chased for 2 h at 19°C. The medium was replaced with prewarmed chase medium, and the cells were incubated at 37°C for the indicated times. Cells were rapidly chilled, treated with trypsin, and quenched with soybean trypsin inhibitor. After solubilization and immunoprecipitation of HA, the kinetics of *trans*-Golgi network-to-cell surface delivery were analyzed by SDS-PAGE and quantitated using a phosphorimager. AMT, amantadine. *B*: HA delivery in CFPAC cells is stimulated by FSK. Cells were infected with AV-M2rev or AV-M2901 and induced as described in *A*. On the following day, cells were starved, radiolabeled for 15 min, and then chased for 2 h at 19°C. FSK (10 μM) was added to the indicated samples starting 10 min before the end of the 19°C incubation. The medium was replaced with prewarmed chase medium (±FSK), the cells were incubated at 37°C, and HA delivery to the cell surface was quantitated as described in *A*. Similar results were obtained in 3 experiments.

or CFTR expression on the recycling of preinternalized $^{125}$I-Tf in polarized CFPAC cells. Using this assay, which is a very sensitive reporter for changes in endosomal pH, we found no effect of M2 or CFTR, even when they were expressed at a very high MOI (Fig. 10). Thus our data suggest that CFTR does not regulate organelle pH or membrane trafficking in polarized epithelial cells.

## DISCUSSION

Many organelles in the secretory pathway are acidified by electrogenic proton-translocating ATPases. As these ATPases pump protons into the lumen of an organelle, they generate a membrane potential gradient that inhibits further acidification. In normal cells, this membrane potential is collapsed by a parallel chloride conductance, allowing maximal acidification (1, 3, 24). The acidification hypothesis suggests that CFTR may play this role in the late Golgi and endosomal compartments of epithelial cells. The original studies by Barasch et al. (2, 4) used the membrane permeant weak base DAMP to estimate that the pH of the TGN and endosomes in several CF cell lines (including immortalized respiratory epithelia and the pancreatic adenocarcinoma line CFPAC-1) and primary cultures (from nasal polyps) was elevated by ~0.2 pH units compared with controls. Furthermore, they showed that a light vesicle fraction isolated from CF cells was slow to acidify compared with that from normal cells and that degradation of internalized endocytosed $\alpha_2$-macroglobulin was delayed significantly in CF compared with normal cells, although lysosomal pH was unaltered (4). Together, these data suggested that CFTR plays a role in regulating and maintaining the pH of the TGN and endosomes.

CFTR has been localized to endocytic compartments and found to recycle from the plasma membrane in several cell types (6, 7, 44, 55, 76). Moreover, although

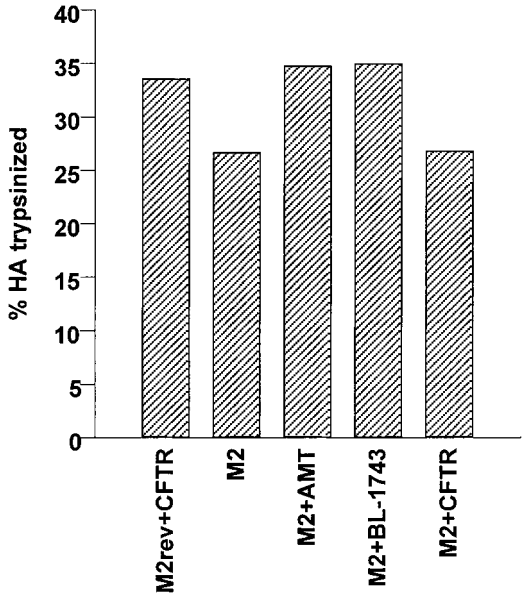


Fig. 8. CFTR expression does not reverse the effect of M2 on HA cell surface delivery in CFPAC cells. CFPAC cells were infected with the indicated adenoviruses in addition to AV-TA. On the following day, the HA was starved, radiolabeled for 15 min, chased for 2 h at 19°C, and then warmed to 37°C for 1 h, and the amount of HA at the cell surface was quantitated as described in MATERIALS AND METHODS. M2 ion channel inhibitors AMT and BL-1743 were included where indicated. CFTR expression had no effect on the M2-mediated delay in HA cell surface delivery, whereas inclusion of either AMT or BL-1743 blocked the effect of M2. Similar results were obtained in 4 experiments.

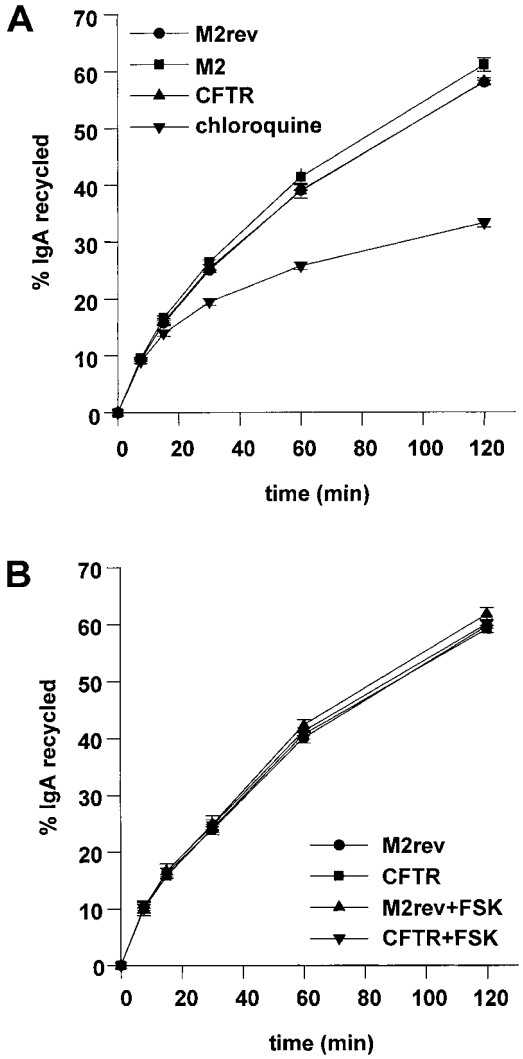


Fig. 9. CFTR expression does not affect apical recycling in CFPAC. *A*: CFPAC cells were infected with AV-TA (MOI 100), AV-pIgR (MOI 250), and AV-M2rev, AV-M2901, or AV-M2 (MOI 250 each) and then induced with 2 mM butyrate. Indicated samples were incubated with 200 μg/ml chloroquine starting 2 h before the experiment. Recycling of preinternalized $^{125}$I-IgA was quantitated the following day as described in MATERIALS AND METHODS. *B*: FSK does not affect IgA exocytosis in CFPAC cells. Cells were infected as described in *A*. Where indicated, FSK (10 μM) was added during the last 10 min of radioligand uptake and in subsequent steps. The rate of $^{125}$I-IgA recycling in FSK-stimulated or nonstimulated cells was unaffected by either M2 or M2901 expression. Values are means ± SD for triplicate samples. Similar results were obtained in at least 4 experiments for each condition.

CFTR has not been localized directly to the Golgi complex, it is not unreasonable to suppose its presence there at steady state. Many recycling proteins and mucins transiently pass through the *trans*-Golgi or TGN as monitored by their repeated exposure to glycosyltransferases (43, 69). In addition, the half-life of mature CFTR is ~7–8 h (75), which is relatively short for an apical membrane protein (66). Therefore, there is likely to be a small amount of newly synthesized CFTR traversing the secretory pathway at any given time. Because CFTR is functional in the endoplasmic reticulum (53), the newly synthesized protein may be active as it transits the Golgi. By contrast, the most common mutant of CFTR (CFTR ΔF508) is retained in the endoplasmic reticulum and does not reach the plasma membrane (13, 19). Although a recent report suggests that CFTR ΔF508 can be detected at the plasma membrane in some tissues (41), we did not detect any cAMP-stimulated halide efflux in mock-infected CFPAC cells by using a highly sensitive assay. Moreover, these cells are thought to express little or no CFTR ΔF508 protein. Thus it is very unlikely that these cells express functional CFTR in endocytic or Golgi compartments.

The goal of our studies was to determine whether CFTR regulates organelle pH in polarized epithelial cells. The acidification hypothesis predicts that the pH of the TGN and apical endosomes, two compartments that should contain CFTR at steady state, is disrupted in CF cells. To test this hypothesis, we developed a model system to selectively disrupt the pH of these two compartments by expression of influenza M2 protein and compared the effects of M2 and CFTR expression in polarized cells. Although M2 activity disrupted protein export from the TGN as well as the trafficking of transcytosing and recycling proteins at the apical surface of polarized MDCK cells, expression of CFTR had no effect on any of these pathways. Furthermore, expression of functional CFTR in a polarized CF cell line did not affect these trafficking steps. Finally, coexpression of CFTR was unable to reverse the effects of M2 on trafficking. Together, our data suggest that *1*) perturbation of TGN and endocytic pH disrupts protein traffic, *2*) TGN pH in CFPAC cells is normally acidic, and *3*) CFTR does not regulate TGN or endosome pH in MDCK or CFPAC cells.

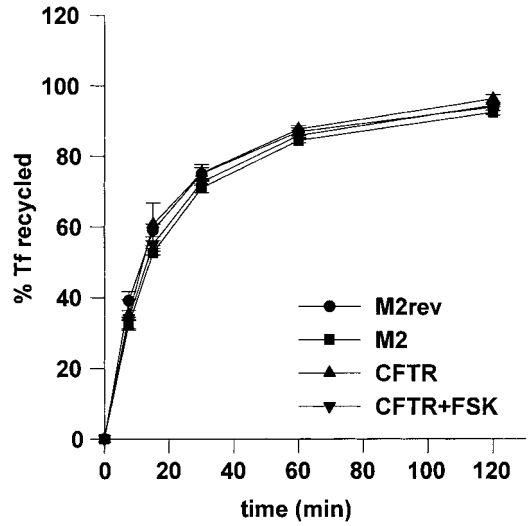


Fig. 10. CFTR expression does not affect recycling of transferrin (Tf) in CFPAC. CFPAC cells were infected with AV-TA (MOI 200) and AV-M2rev, AV-M2, or AV-M2901 (MOI 2,500). FSK was added to the indicated samples during the $^{125}$I-Tf uptake and in subsequent steps. The rate of $^{125}$I-Tf recycling was determined as described in MATERIALS AND METHODS. Values are means ± SD for triplicate samples. Similar results were obtained in 2 experiments.

Several studies by other groups have also failed to observe any effects of CFTR on organelle pH or protein trafficking. For example, no significant elevation in the pH of endosomes was observed when CFTR was transfected into Chinese hamster ovary, 3T3, or L cells (7, 20, 44, 57, 58, 62). However, these cells do not normally express functional CFTR and likely have other functional chloride conductances that regulate organelle pH. Therefore, heterologous expression of CFTR in these cells is unlikely to disrupt normal pH regulation. Interestingly, one study found that CFTR expression in 3T3 cells stimulated endosome fusion (6); this is an intriguing observation because regulation of endosome fusion requires acidification and appears to be regulated by membrane potential (28). Thus it is possible that CFTR expression could alter membrane potential in endosomes without affecting pH. Another study found no effect of CFTR expression on the kinetics of transferrin recycling or on endosomal pH in isolated CFPAC cells (21). However, because transferrin recycles almost exclusively from the basolateral surface in most polarized epithelial cells, an effect of CFTR on trafficking through an apical compartment might have been missed in these studies. Similarly, because the CFPAC cells used in our studies also were not fully polarized, it is possible that they also expressed a redundant counterion conductance that would be absent from apical endocytic compartments in fully polarized cells. Therefore, definitive resolution of the role of CFTR in regulating apical endosome pH awaits the development of well-matched, -characterized, and -polarized CF and rescued epithelial cells.

Recently, the regulation of membrane insertion into and retrieval from the cell surface has been linked to the activation of CFTR (10, 38, 70). Bradbury et al. (10) compared endocytosis and exocytosis in CFPAC cells transfected with CFTR or with vector alone. Under basal conditions the extent of endocytosis of rhodamine dextran was identical in both cell types; however, FSK treatment inhibited endocytosis and stimulated exocytosis only in cells expressing CFTR. Similarly, recycling of preinternalized wheat germ agglutinin was stimulated by FSK in CFTR-expressing cells. This suggests that CFTR activation can modulate membrane recycling in some cells. By contrast, in our experiments, we observed FSK-stimulated exocytosis of newly synthesized HA in CFPAC cells independently of CFTR expression and saw no effect of FSK on the rate of exocytosis of IgA. Although we do not understand the reason for this discrepancy, we can envision several possibilities to explain this difference. First, the corrected CFPACs used by Bradbury et al. (10) were a subclone of the original CFPAC line and might have diverged from the original clone; we have previously (40) demonstrated that even clonally related cell lines can be inappropriate for studying the role of CFTR in protein processing. Thus it is possible that the rescued CFPAC subclone has distinct membrane trafficking properties that are unrelated to expression of wild-type CFTR. Second, our assay measured the effect of CFTR expression on the endocytosis of a specific protein (IgA) that is known to be internalized via clathrin-mediated endocytosis at the apical surface of polarized cells. CFTR has also been demonstrated to be internalized via clathrin-coated vesicles (8, 9). By contrast, the previous study followed the internalization of the rhodamine-dextran and wheat germ agglutinin, which are internalized via both clathrin-dependent and clathrin-independent pathways. Clathrin-independent mediated endocytosis from the apical surface of other polarized epithelial cells is stimulated by FSK (22); thus it is possible that CFTR expression indirectly stimulates the clathrin-independent pathway.

We were surprised to find that expression of M2 had no effect on IgA traffic in CFPAC cells, even when it was expressed at 10-fold higher levels than our usual condition. IgA recycling was slowed by cell treatment with the global pH perturbant chloroquine, suggesting that organelle acidification is important for apical postendocytic traffic in these cells. One possibility is that M2 is not efficiently localized to apical endosomes in these cells. M2 does not contain a functional endocytosis signal (Henkel JR and Weisz OA, unpublished observations); thus its endosomal localization depends on either bulk flow membrane trafficking or transient passage of newly synthesized protein through endosomes en route to the plasma membrane. Although the effects of M2 on apical recycling are maximal at the relatively low expression levels used in this and previous studies (31), it is possible that much higher expression levels are necessary to accumulate M2 in endosomes in CFPAC cells. Alternatively, because the CFPAC cells do not grow as fully polarized monolayers, our "recycling" assay reports a combination of apical recycling, basolateral recycling, and transcytosis. The total uptake and the amount of preinternalized IgA released via these pathways will be different depending on whether a cell is fully polarized or is at the edge of an island of cells. Thus, if basolateral recycling contributes to a majority of the release, an effect of M2 on apical recycling or transcytosis would be masked.

Although there is accumulating evidence against a role for CFTR in the regulation of organelle pH and membrane trafficking, the contribution of CFTR activity to protein processing and glycosylation in the TGN remains unclear (see Ref. 63 for review). Whereas we and others have found no effect of CFTR expression on glycosylation (40, 48, 56), several studies have linked the CF phenotype to increased glycoconjugate sulfation (11, 12, 23, 35, 80). The data presented here suggest that this increase in sulfation is due not to altered TGN pH but, rather, to other defects in CF cells. For example, CFTR has been reported to transport the sulfate donor adenosine-3′-phosphate 5′-phosphosulfate (52), and this could account for the observed defect in sulfation in CF cells. Alternatively, other modifying genes may be responsible for the sulfation defect (79). Thus future studies are needed to address the mechanism by which CFTR may modulate glycoconjugate processing.

We thank Dr. Xiaosui Jiang for performing preliminary experiments, Dr. Robert Lamb, Northwestern University, Evanston, IL, for the gift of monoclonal antibody 5C4, and Dr. Mark Krystal, Bristol-Myers Squibb Pharmaceutical Research Institute, Wallingford, CT, for the gift of M2 ion channel inhibitor BL-1743.

This work was supported by grants from the Cystic Fibrosis Foundation, by National Institute of Diabetes and Digestive and Kidney Diseases (NIDDK) Grant DK-54407 (to O. A. Weisz), and by Dialysis Clinic, Inc. W. G. Hill was supported by NIDDK Grant DK-50829 (to R. A. Frizzell).

## REFERENCES

1. **Al-Awqati Q.** Proton-translocating ATPases. *Annu Rev Cell Biol* 2: 179–199, 1986.
2. **Barasch J and Al-Awqati Q.** Defective acidification of the biosynthetic pathway in cystic fibrosis. *J Cell Sci Suppl* 17: 229–233, 1993.
3. **Barasch J, Gershon MD, Nunez EA, Tamir H, and Al-Awqati Q.** Thyrotropin induces the acidification of the secretory granules of parafollicular cells by increasing the chloride conductance of the granular membrane. *J Cell Biol* 107: 2137–2147, 1988.
4. **Barasch J, Kiss B, Prince A, Saiman L, Gruenert D, and Al-Awqati Q.** Defective acidification of intracellular organelles in cystic fibrosis. *Nature* 352: 70–73, 1991.
5. **Barth AIM, Pollack AL, Altschuler Y, Mostov KE, and Nelson WJ.** $NH_2$-terminal deletion of β-catenin results in stable colocalization of mutant β-catenin with adenomatous polyposis coli protein and altered MDCK cell adhesion. *J Cell Biol* 136: 693–706, 1997.
6. **Biwersi J, Emans N, and Verkman AS.** Cystic fibrosis transmembrane conductance regulator stimulates endosome fusion in vivo. *Proc Natl Acad Sci USA* 93: 12484–12489, 1996.
7. **Biwersi J and Verkman AS.** Functional CFTR in endosomal compartment of CFTR-expressing fibroblasts and T84 cells. *Am J Physiol Cell Physiol* 266: C149–C156, 1994.
8. **Bradbury NA, Clark JA, Watkins SC, Widnell CC, Smith HS, and Bridges RJ.** Characterization of the internalization pathways for the cystic fibrosis transmembrane conductance regulator. *Am J Physiol Lung Cell Mol Physiol* 276: L659–L668, 1999.
9. **Bradbury NA, Cohn JA, Venglarik CJ, and Bridges RJ.** Biochemical and biophysical identification of cystic fibrosis transmembrane conductance regulator chloride channels as components of endocytic clathrin-coated vesicles. *J Biol Chem* 269: 8296–8302, 1994.
10. **Bradbury NA, Jilling T, Berta G, Sorscher EJ, Bridges RJ, and Kirk KL.** Regulation of plasma membrane recycling by CFTR. *Science* 256: 530–532, 1992.
11. **Carnoy C, Ramphal R, Scharfman A, Lo-Guidice J-M, Houdret N, Klein A, Galabert C, Lamblin G, and Roussel P.** Altered carbohydrate composition of salivary mucins from patients with cystic fibrosis and the adhesion of *Pseudomonas aeruginosa*. *Am J Respir Cell Mol Biol* 9: 323–334, 1993.
12. **Cheng PW, Boat TF, Cranfill K, Yankaskas JR, and Boucher RC.** Increased sulfation of glycoconjugates by cultured nasal epithelial cells from patients with cystic fibrosis. *J Clin Invest* 84: 68–72, 1989.
13. **Cheng SH, Gregory RJ, Marshall J, Paul S, Souza DW, White GA, O'Riordan CR, and Smith AE.** Defective intracellular transport and processing of CFTR is the molecular basis of most cystic fibrosis. *Cell* 63: 827–834, 1990.
14. **Chizhmakov IV, Geraghty FM, Ogden DC, Hayhurst A, Antoniou M, and Hay AJ.** Selective proton permeability and pH regulation of the influenza M2 channel expressed in mouse erythroleukaemia cells. *J Physiol (Lond)* 494: 329–336, 1996.
15. **Ciampor F, Bayley PM, Nermut MV, Hirst EMA, Sugrue RJ, and Hay AJ.** Evidence that the amantadine-induced, M2-mediated conversion of influenza virus A virus hemagglutinin to the low pH conformation occurs in an acidic trans Golgi compartment. *Virology* 188: 14–24, 1992.
16. **Clague MJ, Urbe S, Aniento F, and Gruenberg J.** Vacuolar ATPase activity is required for endosomal carrier vesicle formation. *J Biol Chem* 269: 21–24, 1994.
17. **Davies JC, Stern M, Dewar A, Caplen NJ, Munkonge FM, Pitt T, Sorgi F, Huang L, Bush A, Geddes DM, and Alton EWFW.** CFTR gene transfer reduces the binding of *Pseudomonas aeruginosa* to cystic fibrosis respiratory epithelium. *Am J Respir Cell Mol Biol* 16: 657–663, 1997.
18. **Demaurex N, Furuya W, D'Souza S, Bonifacino JS, and Grinstein S.** Mechanism of acidification of the trans-Golgi network (TGN). In situ measurements of pH using retrieval of TGN38 and furin from the cell surface. *J Biol Chem* 273: 2044–2051, 1998.
19. **Denning GM, Ostedgaard LS, and Welsh MJ.** Abnormal localization of cystic fibrosis transmembrane conductance regulator in primary cultures of cystic fibrosis airway epithelia. *J Cell Biol* 118: 551–559, 1992.
20. **Dho S, Grinstein S, and Foskett JK.** Plasma membrane recycling in CFTR-expressing CHO cells. *Biochim Biophys Acta* 1225: 78–82, 1993.
21. **Dunn KW, Park J, Semrad CE, Gelman DL, Shevell T, and McGraw TE.** Regulation of endocytic trafficking and acidification are independent of the cystic fibrosis transmembrane regulator. *J Biol Chem* 269: 5336–5345, 1994.
22. **Eker P, Kaae Holm P, van Deurs B, and Sandvig K.** Selective regulation of apical endocytosis in polarized Madin-Darby canine kidney cells by mastoparan and cAMP. *J Biol Chem* 269: 18607–18615, 1994.
23. **Frates RC, Kaizu TT, and Last JA.** Mucus glycoproteins secreted by respiratory epithelial tissue from cystic fibrosis patients. *Pediatr Res* 17: 30–34, 1983.
24. **Glickman J, Croen K, Kelly S, and Al-Awqati Q.** Golgi membranes contain an electrogenic $H^+$ pump in parallel to a chloride conductance. *J Cell Biol* 97: 1303–1308, 1983.
25. **Gossen M and Bujard H.** Tight control of gene expression in mammalian cells by tetracycline-responsive promoters. *Proc Natl Acad Sci USA* 89: 5547–5551, 1992.
26. **Grambas S, Bennett MS, and Hay AJ.** Influence of amantadine resistance mutations on the pH regulatory function of the M2 protein of influenza A viruses. *Virology* 191: 541–549, 1992.
27. **Grambas S and Hay AJ.** Maturation of influenza A virus hemagglutinin–estimates of the pH encountered during transport and its regulation by the M2 protein. *Virology* 190: 11–18, 1992.
28. **Hammond TG, Goda FO, Navar GL, Campbell WC, Majewski RR, Galvan DL, Pontillon F, Kaysen JH, Goodwin TJ, Paddock SW, and Verroust PJ.** Membrane potential mediates $H^+$-ATPase dependence of "degradative pathway" endosomal fusion. *J Membr Biol* 162: 157–167, 1998.
29. **Hansen SH and Casanova JE.** $G_s\alpha$ stimulates transcytosis and apical secretion in MDCK cells through cAMP and protein kinase A. *J Cell Biol* 126: 677–687, 1994.
30. **Hay AJ, Wolstenholme AJ, Skehel JJ, and Smith MH.** The molecular basis of the specific anti-influenza action of amantadine. *EMBO J* 4: 3021–3024, 1985.
31. **Henkel JR, Apodaca G, Altschuler Y, Hardy S, and Weisz OA.** Selective perturbation of apical membrane traffic by expression of influenza virus M2, an acid-activated ion channel, in polarized Madin-Darby canine kidney cells. *Mol Biol Cell* 8: 2477–2490, 1998.
32. **Henkel JR, Gibson GA, Poland PA, Ellis MA, Hughey RP, and Weisz OA.** Influenza M2 proton channel activity selectively inhibits TGN release of apical membrane and secreted proteins in polarized MDCK cells. *J Cell Biol* 148: 495–504, 2000.
33. **Henkel JR, Popovich JL, Gibson GA, Watkins SC, and Weisz OA.** Selective perturbation of early endosome and/or *trans*-Golgi network pH but not lysosome pH by dose-dependent expression of influenza M2 protein. *J Biol Chem* 274: 9854–9860, 1999.
34. **Henkel JR and Weisz OA.** Influenza virus M2 protein slows traffic along the secretory pathway: pH perturbation of acidified compartments affects early Golgi transport steps. *J Biol Chem* 273: 6518–6524, 1998.
35. **Hill WG, Harper GS, Rozakis T, Boucher RC, and Hopwood JJ.** Organ-specific over-sulfation of glycosaminoglycans and altered extracellular matrix in a mouse model of cystic fibrosis. *Biochem Mol Med* 62: 113–122, 1997.

36. **Howard M, DuVall MD, Devor DC, Dong J, Henze K, and Frizzell RA.** Epitope tagging permits cell surface detection of functional CFTR. *Am J Physiol Cell Physiol* 269: C1565–C1576, 1995.
37. **Howard M, Jiang X, Beer Stolz D, Hill WG, Johnson JA, Watkins SC, Frizzell RA, Bruton CM, Robbins PD, and Weisz OA.** Forskolin-induced apical membrane insertion of virally-expressed, epitope-tagged CFTR in polarized MDCK cells. *Am J Physiol Cell Physiol* 279: C375–C382, 2000.
38. **Howard M, Jilling T, DuVall M, and Frizzell RA.** cAMP-regulated trafficking of epitope-tagged CFTR. *Kidney Int* 49: 1642–1648, 1996.
39. **Imundo L, Barasch J, Prince A, and Al-Awqati Q.** Cystic fibrosis epithelial cells have a receptor for pathogenic bacteria on their apical surface. *Proc Natl Acad Sci USA* 92: 3019–3023, 1995.
40. **Jiang X, Hill WG, Pilewski JM, and Weisz OA.** Glycosylation differences between a cystic fibrosis and rescued airway cell line are not CFTR dependent. *Am J Physiol Lung Cell Mol Physiol* 273: L913–L920, 1997.
41. **Kalin N, Claass A, Sommer M, Puchelle E, and Tummler B.** ΔF508 CFTR protein expression in tissues from patients with cystic fibrosis. *J Clin Invest* 103: 1379–1389, 1999.
42. **Lamb RA and Choppin PW.** Identification of a second protein ($M_2$) encoded by RNA segment of influenza virus. *Virology* 112: 729–737, 1981.
43. **Litvinov SV and Hilkens J.** The epithelial sialomucin, episialin, is sialylated during recycling. *J Biol Chem* 268: 21364–21371, 1993.
44. **Lukacs GL, Chang X-B, Kartner N, Rotstein OD, Riordan JR, and Grinstein S.** The cystic fibrosis transmembrane regulator is present and functional in endosomes. Role as a determinant of endosomal pH. *J Biol Chem* 267: 14568–14572, 1992.
45. **Matlin KS and Simons K.** Reduced temperature prevents transfer of a membrane glycoprotein to the cell surface but does not prevent terminal glycosylation. *Cell* 34: 233–243, 1983.
46. **Mohamed A, Ferguson D, Seibert FS, Cai H, Kartner N, Grinstein S, Riordan JR, and Lukacs GL.** Functional expression and apical localization of the cystic fibrosis transmembrane conductance regulator in MDCK I cells. *Biochem J* 322: 259–265, 1997.
47. **Muroi M, Shiragami N, Nagao K, Yamasaki M, and Takatsuki A.** Folimycin (concanamycin A), a specific inhibitor of V-ATPase, blocks intracellular translocation of the glycoprotein of vesicular stomatitis virus before arrival to the Golgi apparatus. *Cell Struct Funct* 18: 139–149, 1993.
48. **Neutra MR, Grand RJ, and Trier JS.** Glycoprotein synthesis, transport, and secretion by epithelial cells of human rectal mucosa. *Lab Invest* 36: 535–546, 1977.
49. **Oda K, Nishimura Y, Ikehara Y, and Kato K.** Bafilomycin $A_1$ inhibits the targeting of lysosomal acid hydrolases in cultured hepatocytes. *Biochem Biophys Res Commun* 178: 369–377, 1991.
50. **Ohuchi M, Cramer A, Vey M, Ohuchi R, Garten W, and Klenk H-D.** Rescue of vector-expressed fowl plague virus hemagglutinin in biologically active form by acidotropic agents and coexpressed $M_2$ protein. *J Virol* 68: 920–926, 1994.
51. **Palokangas H, Metsikko K, and Vaananen K.** Active vacuolar $H^+$ATPase is required for both endocytic and exocytic processes during viral infection of BHK-21 cells. *J Biol Chem* 269: 17577–17585, 1994.
52. **Pasyk EA and Foskett JK.** CFTR is permeable to adenosine 3′-phosphate 5′-phosphosulfate (PAPS). *Pediatr Pulmonol Suppl* 12: LB25, 1995.
53. **Pasyk EA and Foskett JK.** Mutant (ΔF508) cystic fibrosis transmembrane conductance regulator $Cl^-$ channel is functional when retained in endoplasmic reticulum of mammalian cells. *J Biol Chem* 270: 12347–12350, 1995.
54. **Pinto LH, Holsinger LJ, and Lamb RA.** Influenza virus $M_2$ protein has ion channel activity. *Cell* 69: 517–528, 1992.
55. **Prince LS, Workman RB, and Marchase RB.** Rapid endocytosis of the cystic fibrosis transmembrane conductance regulator chloride channel. *Proc Natl Acad Sci USA* 91: 5192–5196, 1994.
56. **Reid CJ, Burdick MD, Hollingsworth MA, and Harris A.** CFTR expression does not influence glycosylation of an epitope-tagged MUC1 mucin in colon carcinoma cell lines. *Glycobiology* 9: 389–398, 1999.
57. **Rodriguez-Boulan E and Pendergast M.** Polarized distribution of viral envelope proteins in the plasma membrane of infected epithelial cells. *Cell* 20: 45–54, 1980.
58. **Root KV, Engelhardt JF, Post M, Wilson JM, and van Dyke RW.** CFTR does not alter acidification of L cell endosomes. *Biochem Biophys Res Commun* 205: 396–401, 1995.
59. **Saiman L, Cacalano G, Gruenert D, and Prince A.** Comparison of adherence of *Pseudomonas aeruginosa* to respiratory epithelial cells from cystic fibrosis patients and healthy subjects. *Infect Immun* 60: 2808–2814, 1992.
60. **Saiman L and Prince A.** *Pseudomonas aeruginosa* pili bind to asialoGM1 which is increased on the surface of cystic fibrosis epithelial cells. *J Clin Invest* 92: 1875–1880, 1993.
61. **Sakaguchi T, Leser GP, and Lamb RA.** The ion channel activity of the influenza virus $M_2$ protein affects transport through the Golgi apparatus. *J Cell Biol* 133: 733–747, 1996.
62. **Santos GF and Reenstra WW.** Activation of the cystic fibrosis transmembrane regulator by cyclic AMP is not correlated with inhibition of endocytosis. *Biochim Biophys Acta* 1195: 96–102, 1994.
63. **Scanlin TF and Glick MC.** Terminal glycosylation in cystic fibrosis. *Biochim Biophys Acta* 1455: 241–253, 1999.
64. **Schoumacher RA, Ram J, Iannuzzi MC, Bradbury NA, Wallace RW, Hon CT, Kelly DR, Schmid SM, Gelder FB, Rado TA, and Frizzell RA.** A cystic fibrosis pancreatic adenocarcinoma cell line. *Proc Natl Acad Sci USA* 87: 4012–4016, 1990.
65. **Schultz BD, Takahashi A, Liu C, Frizzell RA, and Howard M.** FLAG epitope positioned in an external loop preserves normal biophysical properties of CFTR. *Am J Physiol Cell Physiol* 273: C2080–C2089, 1997.
66. **Scott LJ and Hubbard AL.** Dynamics of four rat liver plasma membrane proteins and polymeric IgA receptor. Rates of synthesis and selective loss into the bile. *J Biol Chem* 267: 6099–6106, 1992.
67. **Seksek O, Biwersi J, and Verkman AS.** Evidence against defective *trans*-Golgi acidification in cystic fibrosis. *J Biol Chem* 271: 15542–15548, 1996.
68. **Shimbo K, Brassard DL, Lamb RA, and Pinto LH.** Ion selectivity and activation of the $M_2$ ion channel of influenza virus. *Biophys J* 70: 1335–1346, 1996.
69. **Snider MD.** Remodeling of glycoprotein oligosaccharides after endocytosis: a measure of transport into compartments of the secretory apparatus. *Methods Cell Biol* 32: 339–350, 1989.
70. **Takahashi A, Watkins SC, Howard M, and Frizzell RA.** CFTR-dependent membrane insertion is linked to stimulation of the CFTR chloride conductance. *Am J Physiol Cell Physiol* 271: C1887–C1894, 1996.
71. **Takeuchi K and Lamb RA.** Influenza virus $M_2$ protein ion channel activity stabilizes the native form of fowl plague virus hemagglutinin during intracellular transport. *J Virol* 68: 911–919, 1994.
72. **Tu Q, Pinto LH, Luo G, Shaughnessy MA, Mullaney D, Kurtz S, Krystal M, and Lamb RA.** Characterization of inhibition of $M_2$ ion channel activity by BL-1743, an inhibitor of influenza A virus. *J Virol* 70: 4246–4252, 1996.
73. **Van Weert AWM, Dunn KW, Geuze HJ, Maxfield FR, and Stoorvogel W.** Transport from late endosomes to lysosomes, but not sorting of integral membrane proteins in endosomes, depends on the vacuolar proton pump. *J Cell Biol* 130: 821–834, 1995.
74. **Wang C, Lamb RA, and Pinto LH.** Direct measurement of the influenza A virus $M_2$ protein ion channel activity in mammalian cells. *Virology* 205: 133–140, 1994.
75. **Ward CL and Kopito RR.** Intracellular turnover of cystic fibrosis transmembrane conductance regulator. *J Biol Chem* 269: 25710–25718, 1994.
76. **Webster P, Vanacore L, Nairn AC, and Marino CR.** Subcellular localization of CFTR to endosomes in a ductal epithelium. *Am J Physiol Cell Physiol* 267: C340–C348, 1994.

77. **Yilla M, Tan A, Ito K, Miwa K, and Ploegh HL.** Involvement of the vacuolar $H^+$-ATPases in the secretory pathway of HepG2 cells. *J Biol Chem* 268: 19092–19100, 1993.
78. **Yoshimori T, Yamamoto A, Moriyama Y, Futai M, and Tashiro Y.** Bafilomycin $A_1$, a specific inhibitor of vacuolar-type $H^+$ATPase, inhibits acidification and protein degradation in lysosomes of cultured cells. *J Biol Chem* 266: 17707–17712, 1991.
79. **Zhang Y, Doranz B, Yankaskas JR, and Engelhardt JF.** Genotypic analysis of respiratory mucous sulfation defects in cystic fibrosis. *J Clin Invest* 96: 2997–3004, 1995.
80. **Zhang Y, Jiang Q, Dudus L, Yankaskas JR, and Engelhardt JF.** Vector-specific complementation profiles of two independent primary defects in cystic fibrosis airways. *Hum Gene Ther* 9: 635–648, 1998.